Electronic Supplementary Material (ESI) for Journal of Materials Chemistry C.

SUPPLEMENTARY MATERIALS

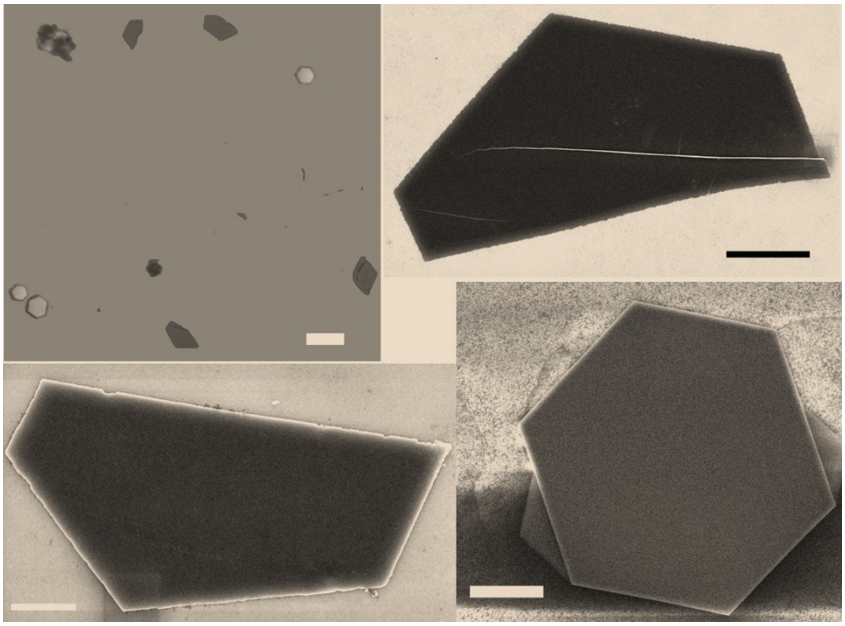

Figure S1. Typical optical (Top left) and SEM images of grown VS_2 flakes. The scale bar is 1 μm.

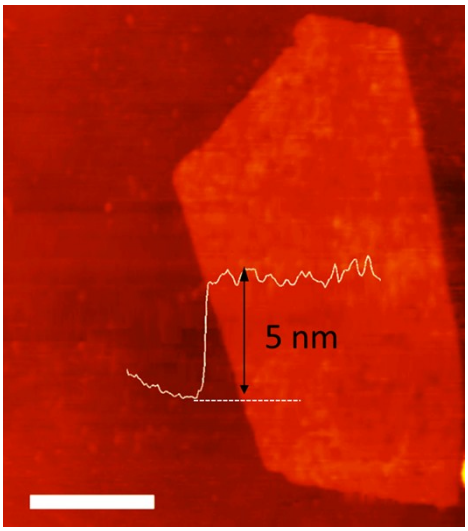

Figure S2. Atomic Force Microscopy of a typical VS_2 flake with a thickness of 5 nm.

Energy-dispersive X-ray spectroscopy (EDS) of VS_2

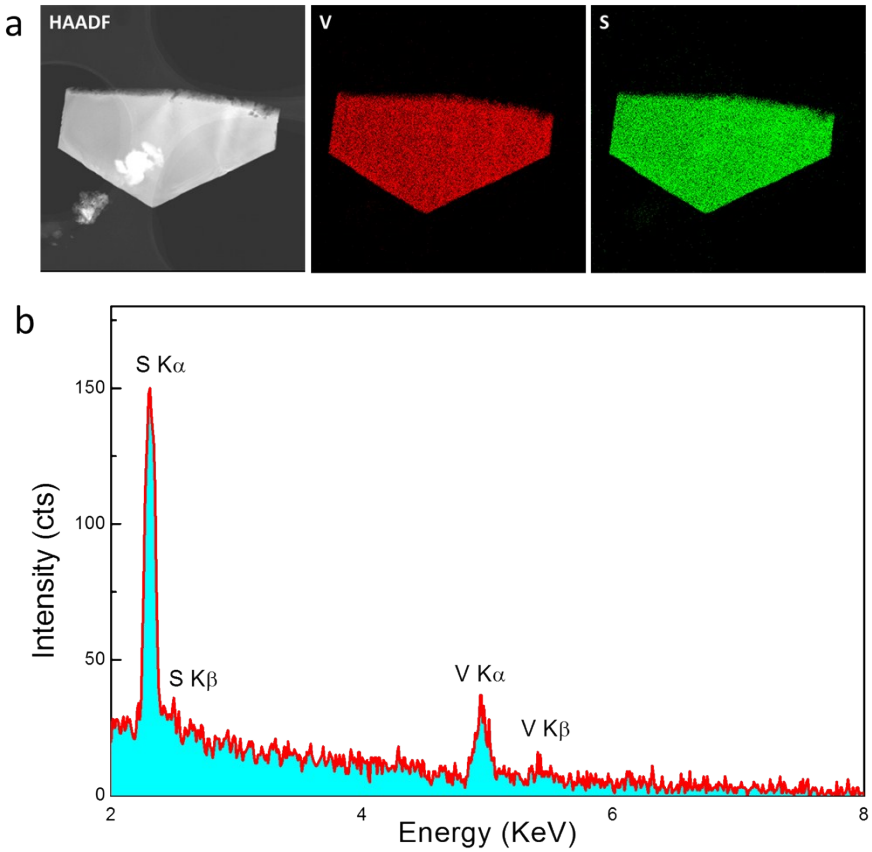

Figure S3. (a) EDS element mapping of VS_2. (b) EDS of VS_2.

Raman characterization of VS_2

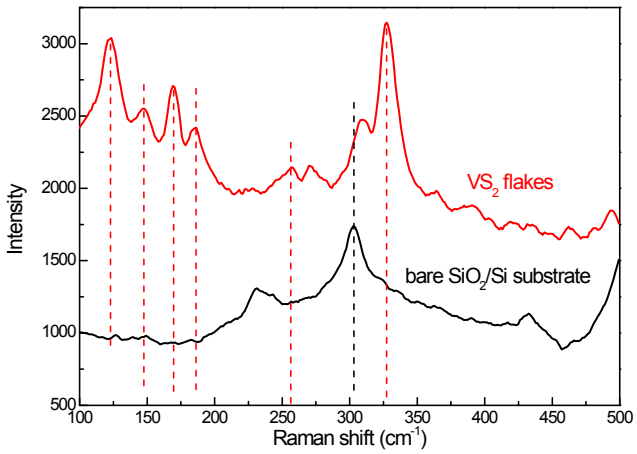

Figure S4. Raman spectra of VS_2 flakes and the bare substrate.

The positioning of the highest peak around 330 cm^{-1} and the wide hump around 260 cm^{-1} agree with the earlier publication, which are tentatively assigned to the out-of-plane (A_1) and in-plane (E_2) vibration modes of VS_2, respectively[1,2]. A series of peaks from 120 cm^{-1} to 190 cm^{-1} are clear in our sample and they were claimed in the Ref. S1 as two-phonon process signals. On the other hand, we note these peaks (120-190 cm^{-1}) are close to the results of calculations of phonons in 1T-VS2 (Ref.S3). It is worth mentioning that all these Raman peaks are quite different from those of V_5S_8 nanosheets (E1a ~280 cm^{-1}, A1a ~ 406 cm^{-1} in Ref.3) although it is also possible that the spectra are influenced by phases of V and S[4].

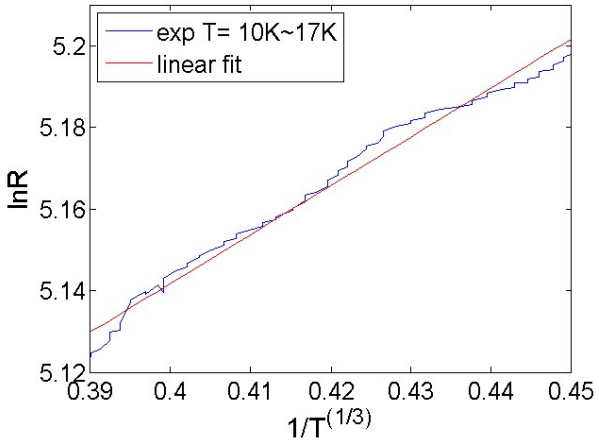

Figure S5. R-T curves. The resistance (R) is fitted for the lowest temperature (T) range 10 ~ 20K. In this range the R-T relation can be fitted by using axes of $\ln R$ and $\left(\frac{1}{T}\right)^{1/3}$ to show linear dependence, demonstrating the good fit of the data to the empirical formula $R(T) = A_0 exp\{\left({T_0}/{T}\right)^{\frac{1}{d+1}}\}$.

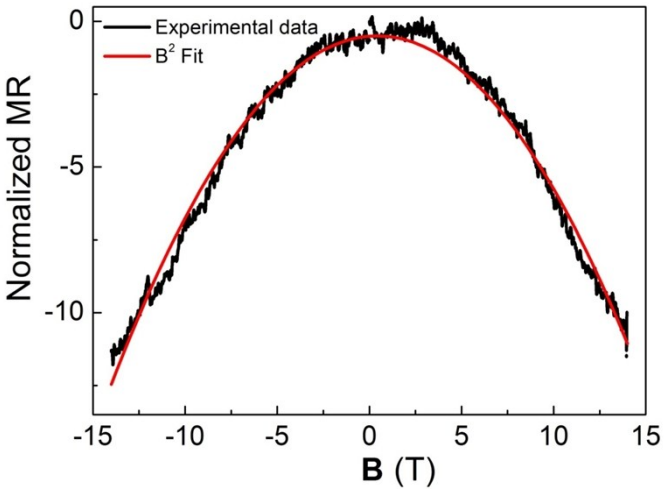

Figure S6 The quadratic **B** fitting for the MR of VS_2 measured at 2K under an in-plane magnetic up to 14T. The strong correlation shows that the MR can be fitted by quadratic **B** quite well.

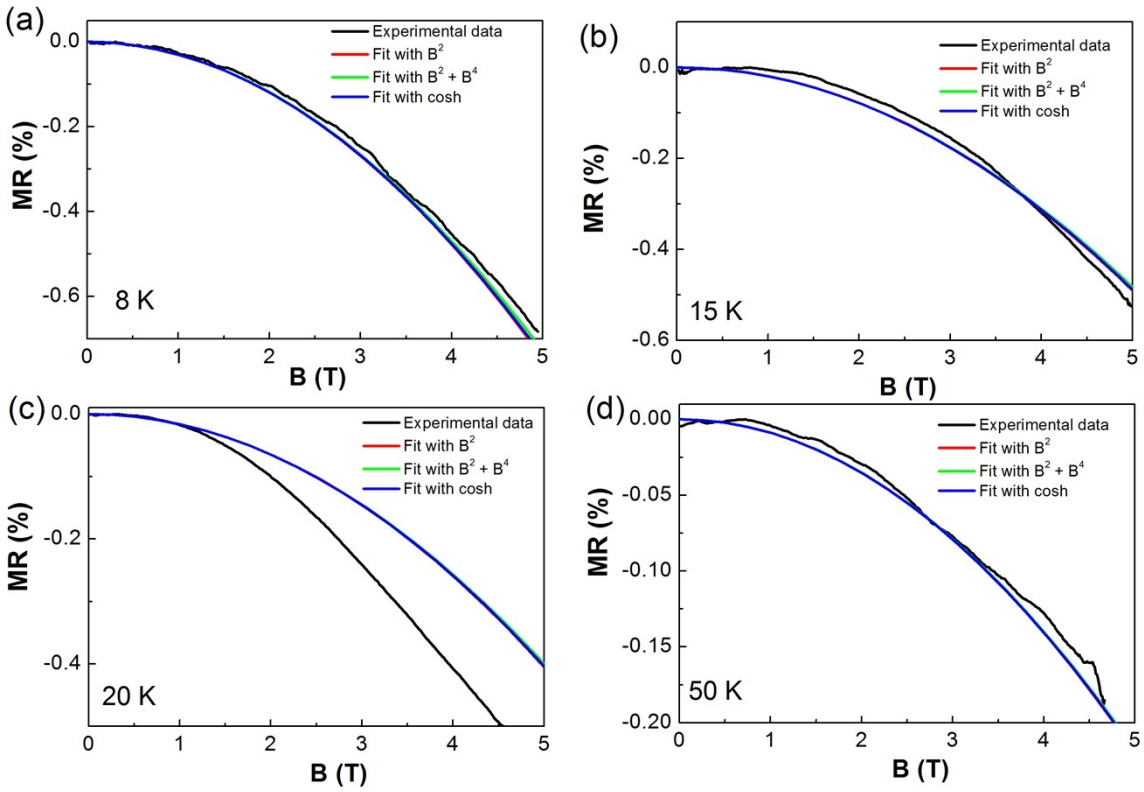

Figure S7 Temperature dependent MR curves fitted considering only the B^2 term, $B^2 + B^4$ term, and the full *cosh* function.

Magnetic crystalline anisotropy energy calculation

The magnetic crystalline anisotropy energy (MAE) is the energy difference of the system when the magnetization is along different directions due to spin-orbit coupling (SOC). The magnetization direction with lower energy is easier to achieve, and hence determines the easy axis, while the direction with higher energy determines the hard axis. Therefore, the MAE can be estimated from the difference between the energies required when applying the magnetic field along different directions to achieve magnetization saturation, starting from a demagnetized state. From the measured normalized hysteresis loop (**Figure 3d**), we can calculate the energy difference of each unit cell by calculating the magnetic energy $\int M\, dB$. It is known that the out of plane magnetisation curve contains a strong demagnetisation energy term and magnetic domains are formed to reduce the demagnetisation energy. Considering the films are uniformly magnetized. The demagnetization field, $4\pi M_s$ will occur in the out-of-plane direction and the effective field along the out-of-plane direction should be $H-4\pi M_s$. Adopting the saturated magnetic moment M_S to be about 0.5 μ_B obtained from the *ab initio* results, and the unit cell volume of VS_2 is 17.24 Å^3 = 1.724 $\times 10^{-23}$ cm^3. Therefore the demagnetization field is equal to 0.33T. After subtracting the contribution of the demagnetization field, we found out the MAE to be about $16.3\ \mu eV$, which is also very close to the value of 19 μeV predicted from *ab initio* results. Therefore, both theory and experiments consistently indicate that VS_2 is a magnetic material.

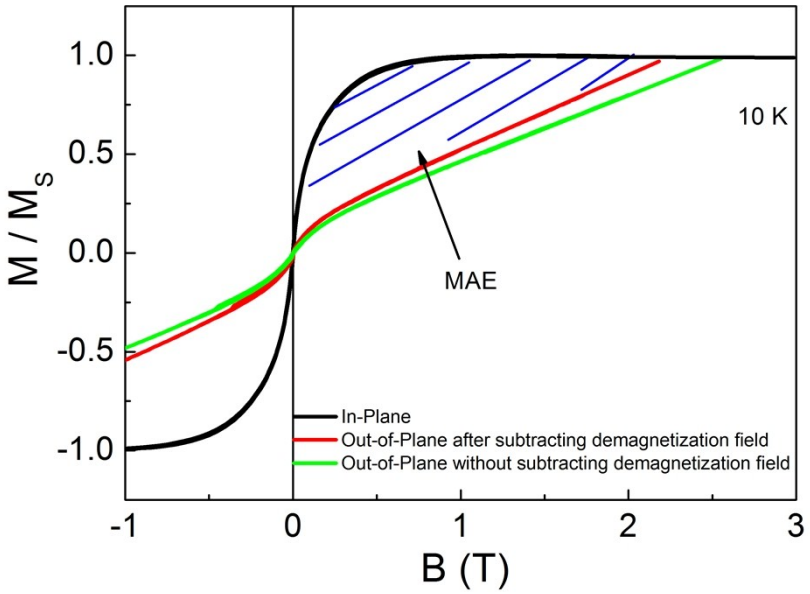

Figure S8. Schematic drawing of MAE calculation.

Anomalous Hall effect of VS_2

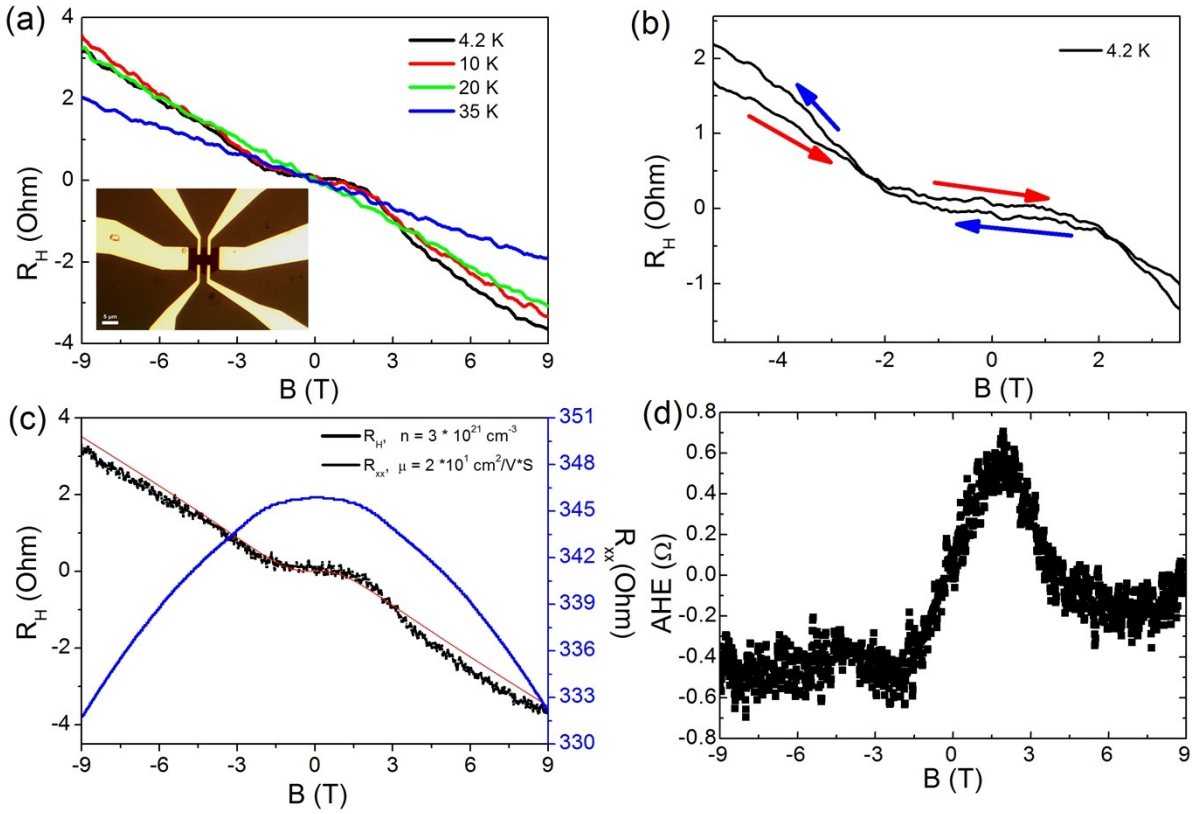

Figure S9. (a) Temperature dependent AHE of VS2 flake. (b) AHE measured at 4.2 K. (c) MR and AHE measured at 4.2K, where AHE is fitted with the two-channel conduction model. (d) AHE after subtracting the linear component due to the conventional Hall effect.

Figure S9a and **S9b** show temperature dependent AHE of a VS_2 flake. The field cycle directions are indicated in **Figure S9b**. One can see that the measured Hall resistance is close to but not zero. There are two main contributions to the measured curve (the conventional Hall effect and anomalous Hall effect), in which the conventional Hall effect contributes to the linear portion at high field. The anomalous Hall effect mainly describes the nonlinear term of the Hall signal, which is usually related to the out-of-plane magnetic moment of the measured sample. To demonstrate that the measured nonlinear curve is not due contributions from multiple bands. We fitted the R_H curve with the two-channel conduction model (**Figure S9c**). However, we could not well reproduce

produce a matching fitting for the data even under the best result (see the red curve above), where these parameters: n_1 = -2.7 * 10^{22} cm^{-3}, μ_1= 0.023 cm^2/VS, n_2 = 0.015 * 10^{21} cm^{-3}, μ_2 = 3926 cm^2/VS, still indicate the major conductance contribution comes from channel 2 (> 99%). In contrast, using the slope of the high-field R_H and only considering one type of carrier (hole), we obtain the values, n = 3*10^{21} cm^{-3}, μ = 20 cm^2/VS, which are more reasonable. Therefore, we believe that the nonlinear Hall resistance is due to the anomalous Hall effect. After subtracting the linear background, we obtain a signal proportional to the magnetic moments in the crystal (**Figure S9d**). The saturation field around 2.6 T is consistent with the M(H) curve we measured, which further reflects the switching of magnetic structure in the crystal.

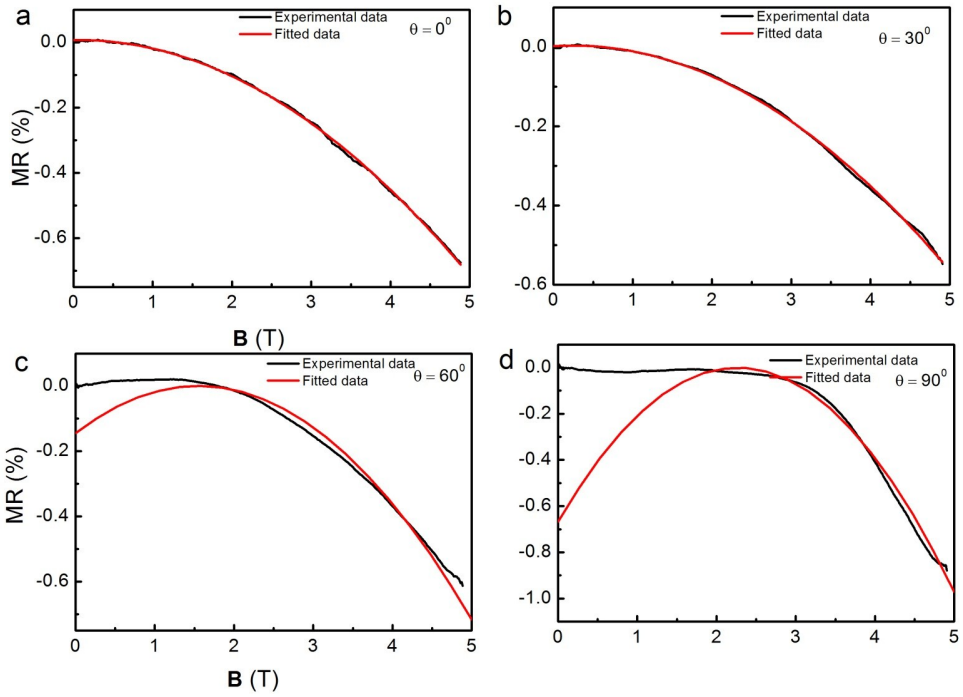

Figure S10 The angular threshold for quadratic dependence of external field of H for NMR of VS_2. The quadratic **B** dependence of MR starts from threshold field $\mathbf{B_c}$. Before $\mathbf{B_c}$, MR is considered to be constant at zero. Different values of the angle θ of magnetic field with respect to the in-plane result in different threshold fields $\mathbf{B_c}$. The threshold field (a) Bc =0, (b) Bc= 0.5667 T, (c) Bc = 1.7 T, and (d) Bc= 2.2667 T.

Lattice Constants used in calculations	[001] (eV)	Magnetic moment (μ_B)	[100](eV)	Magnetic moment (μ_B)	$\Delta E(\mu eV)$=[001]-[100]
Lattice constant and ion positions from Experiment	-20.307726	0.5562	-20.307745	0.5563	19
only ion positions optimization	-20.307958	0.5558	-20.307982	0.5561	24
Lattice constants and ion positions optimization	-20.319442	0.4692	-20.319456	0.4693	14

Table S1. Calculated magnetic anisotropy energies and magnetic moments for three different optimization methods: fixed lattice constants and ion positions from reported experiments, only ion positions relaxed and fixed lattice constants, and lattice constants and ion positions all relaxed.

Supplementary references

1. Yuan, J. *et al.* Facile Synthesis of Single Crystal Vanadium Disulfide Nanosheets by Chemical Vapor Deposition for Efficient Hydrogen Evolution Reaction. *Adv. Mater.* **27**, 5605-5609 (2015).
2. Ji, Q. *et al.* Metallic Vanadium Disulfide Nanosheets as a Platform Material for Multifunctional Electrode Applications. *Nano Letters* **17**, 4908-4916, doi:10.1021/acs.nanolett.7b01914 (2017).
3. Zhang, H., Liu, L.-M. & Lau, W.-M. Dimension-dependent phase transition and magnetic properties of VS 2. *J. Mater. Chem. A* **1**, 10821-10828 (2013).
4. Yang, C. *et al.* V5S8-graphite hybrid nanosheets as a high rate-capacity and stable anode material for sodium-ion batteries. *Energy Environ Sci.* **10**, 107-113, doi:10.1039/C6EE03173K (2017).